Stability of s-band states in the tilting calculation of 1820s

doi: 10.1103/PhysRevC.74.017301

Stability of *s*-band states in the tilting calculation of ^{182}Os

Y. Hashimoto
Graduate School of Pure and Applied Sciences, University of Tsukuba, Tsukuba 305-8571, Japan

T. Horibata
Faculty of Software and Information Technology, Aomori University, Aomori, Aomori 030-0943, Japan

(Received 8 March 2006; published 7 July 2006)

We carried out the three-dimensional cranking calculations for osmium ^{182}Os within the Hartree-Fock-Bogoliubov framework. It turned out that the state in the *g*-band is stable (unstable) with respect to the tilt angle of the cranking axis when the angular momentum is below (above) a critical value. However, the states in the *s*-band with the angular momentum below $30\hbar$ are unstable everywhere along the band. In our model calculations, the wobbling motion does not exist on top of the *s*-band state characterized by the component of two aligned particles.

DOI: 10.1103/PhysRevC.74.017301 PACS number(s): 21.60.−n, 27.70.+q

The investigation of nuclear rotational motion has been one of the central tasks in nuclear many-body problems. The rotational motion is closely related with nuclear shape, because the nuclear collective rotation occurs as a result of restoration process of the broken symmetries in the nuclear mean field.

Within the framework of the nuclear mean-field theories, the cranking model has been widely made use of as a useful tool in understanding the microscopic mechanism of the nuclear rotational motion [1]. In the typical cranking model calculations, the nucleus is assumed to be of prolate (or oblate) shape with axial symmetry, rotating about an axis that is perpendicular to the symmetry axis. This is called the one-dimensional rotation. When the axial symmetry is lost in the nuclear mean-field shape, there occurs another type of rotational motion in which the rotational axis is not parallel with the principal axis (PA) with the largest moment of inertia but fluctuating around the PA [2,3]. This type of rotational motion is called the wobbling motion, which is the dynamical motion of the angular momentum. From the theoretical point of view, much more general type of rotation is expected, where the rotational axis is located completely away from any of the principal axes [4,5]. In this model, there are solutions that represent stationary states with respect to the motion of the angular momentum. The stationary solutions correspond to the local minimum states with respect to the tilt angles. This type of states are already discussed in the tilted axis cranking calculation [3]. Because our stationary solution is a special one of the solutions that is obtained by the fully self-consistent calculation, it is called the tilted axis rotation (TAR) [6].

Recently, the wobbling motion was confirmed experimentally as rotational bands with one and two wobbling phonons in ^{163}Lu [7–9]. Theoretical models and microscopic framework have been proposed to study the microscopic structure of the general type of rotational motions [4–6,10].

Horibata and Onishi (HO) carried out 3D cranking calculations based on the Hartree-Fock-Bogoliubov (HFB) method in ^{182}Os [6,10]. They showed two interesting points: First, around the band crossing region of *g*- and *s*-bands, there occurs the hysteresis in such quantities as energy curves, γ deformations, and pairing gaps. Second, there is the possibility of existence of the TAR solution at a point on the prime meridian (and its partner in the opposite hemishere). In their calculations, when the tilt angle to the north is increased from the equator, the cranking solutions keep the structure of the yrast PA solutions up to some critical angle. Beyond the angle, the structure of the cranking solution is changed from the one whose main component is the *g*-band state to the one with the *s*-band property.

HO adopted the generator coordinate method (GCM) with the purpose of studying the structure change and understanding the mechanism of the wobbling and TAR solutions [10]. To explain what the GCM solutions mean, it is quite necessary to have informations about the PA cranking solutions as well as the solutions with tilted rotational axes. In this brief report, therefore, we outline some results of the cranking calculations with the HFB method in ^{182}Os, putting special emphasis on the stability of the PA cranking solutions with respect to the tilting degree of freedom of the cranking axis. We use the same model space and strength parameters in the Hamiltonian as in Ref. [10], together with more strict convergence condition than the previous calculations. The ambiguity discussed in Ref. [10] in the energies of the *s*-band state and the tilt-back state is eliminated in the present calculations (see Fig. 2(a) in Ref. [10]).

The model Hamiltonian used in the present calculation is the same as is used in HO and is given by

$$\hat{H} = \sum_i \epsilon_i C_i^\dagger C_i - \frac{1}{2}\kappa \sum_{\mu=-2}^{2} (-)^\mu \hat{Q}_{-\mu}\hat{Q}_\mu - \sum_{\tau=p,n} g_\tau \hat{P}_\tau^\dagger \hat{P}_\tau, \tag{1}$$

where ϵ_i stand for the single-particle energies and $C_i^\dagger$ (C_i) are the creation (annihilation) operator for the particle state $|i\rangle$. The parameters κ and g_τ are the interaction strengths for the quadrupole-quadrupole and pairing interactions, respectively. Their values are the same as used in the previous calculations in Ref. [10]. The quadrupole operator $\hat{Q}_\mu$ and pairing operator

$P^\dagger_\tau$ are defined as

$$\hat{Q}_\mu = \sum_{ij} \langle i|r^2 Y_{2\mu}|j\rangle C^\dagger_i C_j, \quad P^\dagger_\tau = \sum_{i_\tau>0} C^\dagger_{i_\tau} C^\dagger_{\bar{i}_\tau}. \tag{2}$$

The wave function $|\Phi(\psi)\rangle$ with the tilt angle ψ is obtained by solving the three-dimensional cranked HFB (3D-CHFB) equation,

$$\delta\langle\Phi(\psi)|\left[\hat{H} - \sum_{k=1}^{3}(\mu_k \hat{J}_k + \xi_k \hat{B}_k) - \sum_{\tau=p,n}\lambda_\tau \hat{N}_\tau\right]|\Phi(\psi)\rangle = 0, \tag{3}$$

where the quantities μ_k, ξ_k, and λ_τ are the Lagrange multipliers to adjust the following constraints:

$$\langle\Phi(\psi)|\hat{J}_k|\Phi(\psi)\rangle = j_k \quad (k = 1, 2, 3), \tag{4}$$

$$\langle\Phi(\psi)|\hat{N}_\tau|\Phi(\psi)\rangle = n_\tau \quad (\tau = p, n), \tag{5}$$

and

$$\langle\Phi(\psi)|\hat{B}_k|\Phi(\psi)\rangle = 0 \quad (k = 1, 2, 3). \tag{6}$$

The tilt angle ψ along the prime meridian is measured from the x axis to the symmetry axis (z axis). The operators $\hat{B}_k$ express three off-diagonal components of the mass-quadrupole tensor in the Cartesian-coordinate representation,

$$\hat{B}_k = \tfrac{1}{2}(\hat{Q}_{ij} + \hat{Q}_{ji}) \quad (ijk \text{ cyclic}). \tag{7}$$

We start with solving the CHFB equation to obtain the set of solutions that are used as the initial conditions in the 3D-CHFB calculation in Eq. (3).

In Fig. 1, the energies of the g-band and the s-band states are displayed with respect to the angular momenta. The states in the g-band are obtained in the increasing order of the angular momenta by starting from the ground state with the angular momentum $J = 0\hbar$. Around $J = 23\hbar$, the g-band ends and abruptly shifts to the s-band. However, when the angular momentum is decreased, starting from the solution with $J = 30\hbar$, the s-band goes down to a point around $J = 15\hbar$, at which the band shifts abruptly to the g-band. Thus, in the segment $15\hbar \leqslant J \leqslant 23\hbar$ of the angular momentum, the two

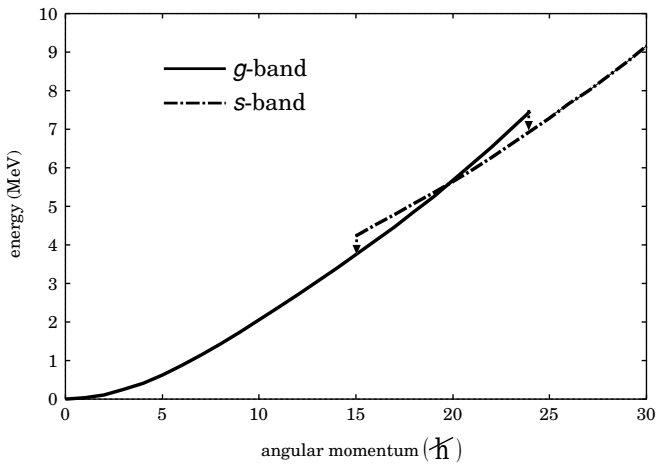

FIG. 1. Plot of energies of g- and s-bands with respect to the angular momentum.

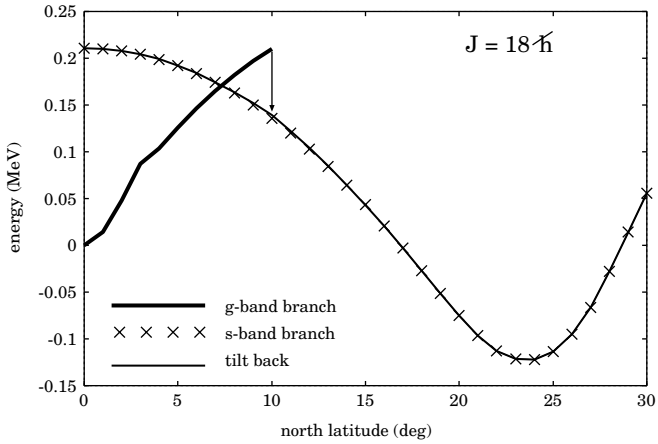

FIG. 2. Energy curves of g- and s-band branches with respect to the tilt angle with angular momentum $J = 18\hbar$. Energies of the states on the curves are the differences from the value of the g-band state at the angle $\psi = 0^\circ$. Thick solid curve is for the g-band branch. The s-band branch is expressed with cross ($\times$) signs. Thin solid curve is obtained by starting from the state at the angle $\psi = 30^\circ$ and decreasing it to zero.

bands with distinct character are located closely in energy to each other. The band crossing takes place around $J = 20\hbar$.

In this band crossing region, a state in the g-band and one in the s-band with the same angular momentum exhibit quite different response to the tilting of the rotational axis along the prime meridian.

In Fig. 2, an example of the energy curves of the states in the g- and s-bands are shown with respect to the tilt angle. The magnitude of the angular momentum is taken to be $J = 18\hbar$. The energy curve that starts from the g-band in the PA cranking (g-band branch) goes up as the tilt angle is increased up to $\psi = 10^\circ$. Then, after passing through the angle $\psi = 10^\circ$, the energy suddenly goes down and the structure of the wave function changes drastically. Increasing the tilt angle further, the energy curve changes smoothly and reaches a minimum point at around $\psi = 23^\circ$. This smooth curve is just the one that starts from the state in the s-band in the PA cranking (s-band branch). This fact is easily seen by carrying out the tilt-back calculation that starts from the state at the tilt angle $\psi = 30^\circ$. At the end of the tilt-back calculation, we arrive at a state just in the s-band with the angle $\psi = 0^\circ$. From the above tilt-up and tilt-back calculations, together with the tilting calculation of the s-band state, we can see that the main component of the wave function of the state on the smooth curve within the tilt angle $0^\circ < \psi < 30^\circ$ is just the same as that of the state in the s-band in the PA cranking. In a similar calculation, HO discussed that a state obtained through the tilt-back process starting from the angle $\psi = 30^\circ$ to 0° might show the s-band character, though its energy was to some extent different from the value of the PA cranking state in the s-band. The present calculation clearly supports their discussions.

According to Refs. [4,5], the TAR is realized when the condition $\boldsymbol{\mu} \times \mathbf{j} = \mathbf{0}$ is satisfied, i.e., the Lagrange multipliers $\boldsymbol{\mu}$ are parallel with the constraints $\mathbf{j}$. We have already illustrated that the condition is satisfied when the TAR solutions are

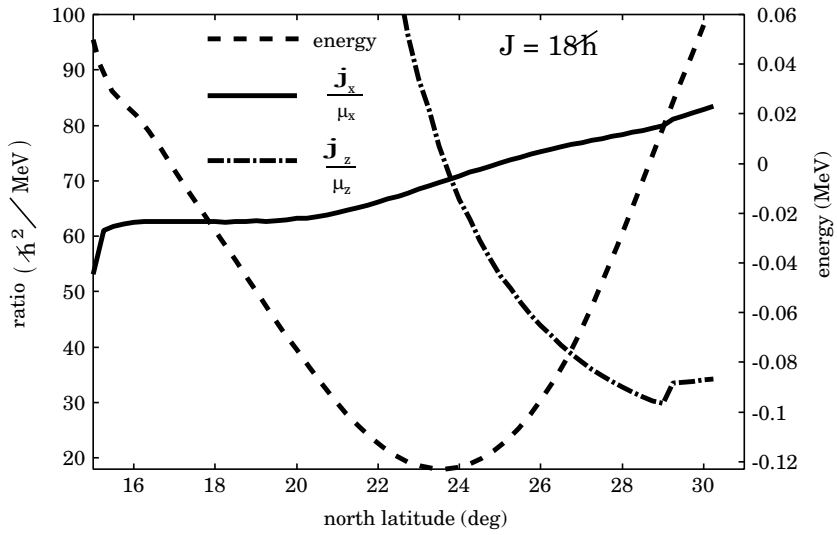

FIG. 3. Plot of j_x/μ_x (solid) and j_z/μ_z (dash-dotted) with respect to tilt angle ψ. The angular momentum is $J = 18\hbar$. Energy curve (right scale) of the s-band branch with $J = 18\hbar$ is also displayed with broken curve for reference.

obtained within the mean field calculations with a simple effective force [11]. In Fig. 3, we show the quantities j_x/μ_x and j_z/μ_z with respect to the tilt angle ψ. The two quantities j_x/μ_x and j_z/μ_z coincide at a value of the tilt angle, just at which the s-band branch has the minimum point. Because the relation $j_x/\mu_x = j_z/\mu_z$ means the angular momentum $\mathbf{j} = (j_x, 0, j_z)$ is parallel with the Lagrange multiplier $\boldsymbol{\mu} = (\mu_x, 0, \mu_z)$, the energy minimum point on the s-band branch corresponds to the TAR.

The most remarkable structure change in the wave functions in the process of the shift from the g-band branch to the s-band one is related with the pairing potential. HO pointed out the "seesaw" mechanism in the structure of the wave functions [10]. When the tilt angle is increased, the proton gap starts with a finite value and gets small rapidly along the g-band branch, being completely zero on the s-band branch. However, the neutron gap stays zero up to the critical tilt angle $\psi = 10^\circ$ on the g-band branch. After passing through the critical angle and shifting to the s-band branch, the neutron gap takes a finite value on the branch. When we come down to tilt angle $\psi = 0^\circ$, contrary to the tilt-up case, the proton gap stays zero and the neutron gap keeps finite value along the s-band branch.

Considering the twofold structure of the phase space near the band crossing region with $J = 20\hbar$, HO predicted the existence of the wobbling motion combined with the g-band branch and the TAR combined with the s-band branch [6]. The wobbling motion is represented by the intersection of the globe of constant angular momentum $j_x^2 + j_y^2 + j_z^2 = J^2$ and the constant energy surface $E(\mathbf{j}) = E_0$ for the given values J and E_0. The visualization of the energy surface around the band crossing region might be useful to understand the property of the wobbling motion as well as the TAR under the angular momentum constraints $j_k (k = 1, 2, 3)$.

In Fig. 4, we show some typical responses in energy of the states in the g- and s-bands with respect to the tilt angle ψ. Each one of the curves in the figure is obtained by tilt-up (F) and tilt-back (B) calculations between the angle $\psi = 0^\circ$ and 30°.

The g-band branch with the angular momentum $J = 16\hbar$ is stable for the angle $0 \leqslant \psi \leqslant 30^\circ$. In the tilt-back

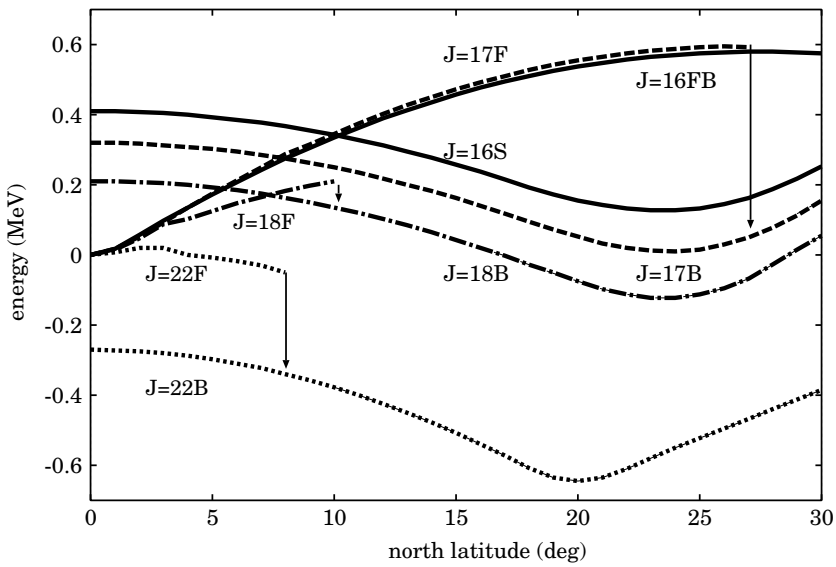

FIG. 4. Energy curves of g- and s-band branches with respect to the tilt angle for the angular momentum values $J = 16\hbar$ (solid), $17\hbar$ (broken), $18\hbar$ (dash-dotted), and $22\hbar$ (dotted). F (B) stands for tilt-up (tilt-back) process with the starting wave function at the angle $\psi = 0^\circ(30^\circ)$, while S means that the branch starts from the state in the s-band at the angle $\psi = 0^\circ$. Displayed energies of the states in the g- and s-band branches for each J are the differences from the energy of the g-band PAR state with the angular momentum J.

calculation, starting from the g-band branch wave function at the angle $\psi = 30^\circ$, we follow the g-band branch curve obtained in the tilt-up calculation back to the g-band state at $\psi = 0^\circ$.

When the angular momentum goes up to $J = 17\hbar$, the g-band branch changes its structure suddenly around the tilt angle $\psi = 27^\circ$ and follows a new smooth curve up to $\psi = 30^\circ$. Tilting back from the wave function at the angle $\psi = 30^\circ$, we get a branch with the s-band nature with a dip around $\psi = 24^\circ$, indicating the existence of the TAR. The height of the minimum is almost the same as the g-band principal axis rotation (PAR) state at $\psi = 0^\circ$. For the angular momentum $J = 18\hbar$, the g-band branch becomes unstable after passing through the angle $\psi = 10^\circ$ and shifts to a new smooth curve obtained in the forward tilting calculation. The new curve, just as in the case with $J = 17\hbar$, turns out to be the s-band branch obtained by tilt-back calculation from the angle $\psi = 30^\circ$. Compared with the g-band branches with $J = 16\hbar$ and $J = 17\hbar$, the g-band branch with $J = 18\hbar$ is shorter in length and lower in height. The height of the dip of the s-band branch is lower than that of the g-band state of the PAR at $\psi = 0^\circ$. This result suggests that the yrast state might be changed from the g-band PAR state to the TAR state with the property of s-band PAR state.

Beyond the band crossing point at the angular momentum $J = 20\hbar$, the situation changes drastically. The g-band branch with $J = 22\hbar$ is almost flat and, after the angle $\psi = 3^\circ$, is bent downward. The length of the g-band is shorter than that with $J = 18\hbar$. It becomes unstable around $\psi = 8^\circ$ and shifts to the s-band branch with the TAR minimum point at $\psi = 20^\circ$. Because the energy of the s-band state of the PAR is lower than that of the g-band state, the TAR minimum is much lower in energy than that of the g-band state of the PAR. In this domain of the angular momentum with the magnitude $J \geqslant 20\hbar$, the TAR is the stable mode of motion, whereas the states in the g- and s-bands are not stable in the tilting calculation.

In relation with the experimental data of the rotational bands with excited wobbling phonon(s), Hamamoto proposed a model that consists of a triaxially deformed core rotor and a particle [9]. According to the model, the core rotor exhibits the wobbling motion on top of the PAR, while the one particle outside the core is kept aligned along an axis (x axis), about which the moment of inertia of the core is the largest. Matsuzaki *et al*. [12,13] pointed out the role played by the aligned particle in determining the condition for the occurrence of the wobbling motion. In the present case, the wobbling motion on top of the g-band state might be expected, which will be discussed by making use of the GCM in a subsequent paper.

Once the tilting degree of freedom is introduced, it turns out, as is shown in Fig. 4, that the state in the s-band is unstable with respect to the tilting of the rotational axis, giving rise to the new stable state of TAR. It is impossible to excite the wobbling motion on a state in the s-band in our calculations with the present Hamiltonian in Eq. (1). The TAR in the present calculations is a stable mode of motion on the s-band branch and plays the role of the yrast state beyond a value of the angular momentum. This case of the TAR with two aligned particles is not a simple extension of the Hamamoto's model with a wobbling core rotor plus aligned *one* particle outside the rotor.

Matsuzaki [14] and Shimizu and Matsuzaki [15] showed the existence of the wobbling motion in osmium ^{182}Os on top of the s-band state in the framework of the random-phase approximation. However, their results oppose our present results. At present, we have no idea which results are more correct, because their model Hamiltonian differes from ours. Furthermore, the dependence of our present results on the parameters in our Hamiltonian should be carefully examined. Studying the similarity and difference among the models adopted in the calculations, it might be possible to extract the essential mechanism which brings about the wobbling motion as well as TAR in the realistic nuclei. It is a challenging and urgent task to establish a microscopic framework to make clear the underlying mechanism of the general three-dimensional nuclear rotational motion. Because the general nuclear rotational motion is a quantum mechanical phenomena, we employ a framework beyond the mean field, i.e., the GCM in our investigations. The results of the GCM calculations will be reported in subsequent papers.

The authors thank Professor N. Onishi for his fruitful discussions and warm encouragement.

[1] P. Ring and P. Schuck, *The Nuclear Many-Body Problem* (Springer-Verlag, New York, 1980).
[2] A. Bohr and B. R. Mottelson, *Nuclear Structure* (Benjamin, New York, 1975), Vol. II.
[3] S. Frauendorf, Rev. Mod. Phys. **73**, 463 (2001).
[4] A. K. Kerman and N. Onishi, Nucl. Phys. **A361**, 179 (1981).
[5] N. Onishi, Nucl. Phys. **A456**, 279 (1986).
[6] T. Horibata and N. Onishi, Nucl. Phys. **A596**, 251 (1996).
[7] S. W. Ødegård *et al*., Phys. Rev. Lett. **86**, 5866 (2001).
[8] D. R. Jensen *et al*., Phys. Rev. Lett. **89**, 142503 (2002).
[9] I. Hamamoto and G. Hagemann, Phys. Rev. C **67**, 014319 (2003).
[10] T. Horibata, M. Oi, N. Onishi, and A. Ansari, Nucl. Phys. **A646**, 277 (1999); **A651**, 435 (1999).
[11] Y. Hashimoto and T. Horibata, Information **8**, 347 (2005).
[12] M. Matsuzaki, Y. R. Shimizu, and K. Matsuyanagi, Phys. Rev. C **65**, 041303(R) (2002).
[13] M. Matsuzaki, Y. R. Shimizu, and K. Matsuyanagi, Phys. Rev. C **69**, 034325 (2004).
[14] M. Matsuzaki, Nucl. Phys. **A509**, 269 (1990).
[15] Y. R. Shimizu and M. Matsuzaki, Nucl. Phys. **A588**, 559 (1996).